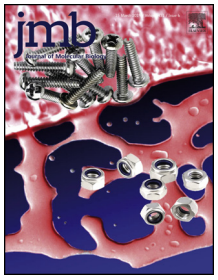

On the Mechanism and Origin of Isoleucyl-tRNA Synthetase Editing against Norvaline

Mirna Bilus[1,†], Maja Semanjski[2,†], Marko Mocibob[1,†], Igor Zivkovic[1], Nevena Cvetesic[3], Dan S. Tawfik[4], Agnes Toth-Petroczy[5], Boris Macek[2] and Ita Gruic-Sovulj[1]

*1 - **Department of Chemistry,** Faculty of Science, University of Zagreb, Zagreb 10000, Croatia*
*2 - **Proteome Center Tuebingen,** University of Tuebingen, Tuebingen 72076, Germany*
*3 - **Institute of Clinical Sciences,** Faculty of Medicine, Imperial College London, and the MRC London Institute of Medical Sciences, London, W12 0NN, United Kingdom*
*4 - **Department of Biomolecular Sciences,** Weizmann Institute of Science, Rehovot 76100, Israel*
*5 - **Max Planck Institute of Molecular Cell Biology and Genetics,** Dresden 01307, Germany*

***Correspondence to Ita Gruic-Sovulj:** Department of Chemistry, Faculty of Science, University of Zagreb, Horvatovac 102a, 10000 Zagreb, Croatia. gruic@chem.pmf.hr*
https://doi.org/10.1016/j.jmb.2019.01.029
Edited by P Wright

Abstract

Aminoacyl-tRNA synthetases (aaRSs), the enzymes responsible for coupling tRNAs to their cognate amino acids, minimize translational errors by intrinsic hydrolytic editing. Here, we compared norvaline (Nva), a linear amino acid not coded for protein synthesis, to the proteinogenic, branched valine (Val) in their propensity to mistranslate isoleucine (Ile) in proteins. We show that in the synthetic site of isoleucyl-tRNA synthetase (IleRS), Nva and Val are activated and transferred to tRNA at similar rates. The efficiency of the synthetic site in pre-transfer editing of Nva and Val also appears to be similar. Post-transfer editing was, however, more rapid with Nva and consequently IleRS misaminoacylates Nva-tRNA^{Ile} at slower rate than Val-tRNA^{Ile}. Accordingly, an *Escherichia coli* strain lacking IleRS post-transfer editing misincorporated Nva and Val in the proteome to a similar extent and at the same Ile positions. However, Nva mistranslation inflicted higher toxicity than Val, in agreement with IleRS editing being optimized for hydrolysis of Nva-tRNA^{Ile}. Furthermore, we found that the evolutionary-related IleRS, leucyl- and valyl-tRNA synthetases (I/L/VRSs), all efficiently hydrolyze Nva-tRNAs even when editing of Nva seems redundant. We thus hypothesize that editing of Nva-tRNAs had already existed in the last common ancestor of I/L/VRSs, and that the editing domain of I/L/VRSs had primarily evolved to prevent infiltration of Nva into modern proteins.

Introduction

The accuracy of protein synthesis (translation) is tightly controlled (error frequency about 10^{-3}–10^{-4}) [1,2]. Key guardians are aminoacyl-tRNA synthetases (aaRSs). These enzymes covalently couple amino acids to their cognate tRNAs (aminoacylation), thus providing the substrates for ribosomal protein synthesis. In principle, there are 20 aaRSs, each specific for one amino acid. Aminoacylation proceeds in two steps (Fig. 1). The amino acid is firstly activated using ATP to form the aminoacyl-adenylate intermediate (aa-AMP; Fig. 1, step 1). In the second step that proceeds in the same active site, the 2′- or 3′-OH group of the terminal adenosine of the tRNA nucleophilically attacks the carbonyl carbon of aa-AMP resulting in transfer of aminoacyl moiety to the tRNA (Fig. 1, step 2). Approximately half of the aaRSs are unable to ensure the required level of specificity in recognition of their amino acid substrates, and may thus activate structurally and chemically similar non-cognate amino acids and transfer them to tRNA. The pool of competing amino acids that a particular aaRS may encounter in the cell consists of both canonical (proteinogenic) and non-canonical (non-proteinogenic) amino acids. The latter

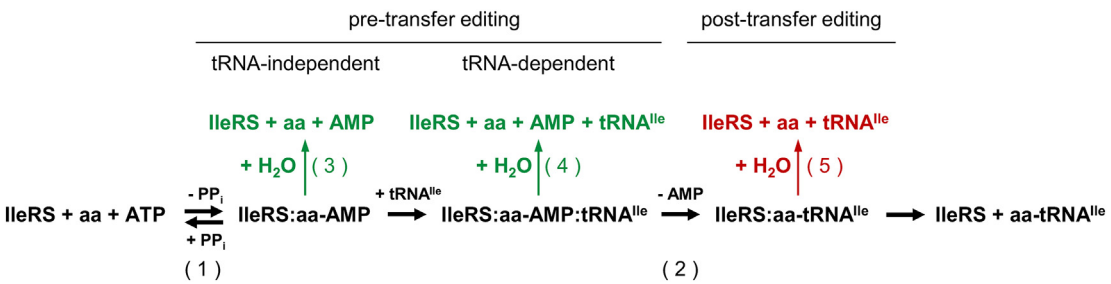

Fig. 1. IleRS pathways of aminoacylation and editing. The synthetic pathway, colored in black, consists of amino acid activation (1) and the aminoacyl transfer step (2). The editing pathways include pre-transfer editing, colored in green, and post-transfer editing, in red. Pre-transfer editing occurs at the synthetic site and comprises the hydrolysis of non-cognate aminoacyl-AMP, which may be tRNA-independent (3) or tRNA-dependent (4). Post-transfer editing regards the hydrolysis of misaminoacylated tRNA (5) at the dedicated editing domain.

are intermediates of metabolic pathways [3] or damaged metabolites [4] that accumulate under various growth/stress conditions [5–8]. To cope with their limited specificity, aaRSs evolved hydrolytic editing to clear their own mistakes in activating and aminoacylating non-cognate amino acids (reviewed in Ref. [9]). Both aminoacyl-AMPs and misaminoacylated tRNAs can be edited. Hydrolysis of aa-AMPs takes place in the same synthetic active site where aa-AMP is formed (pre-transfer editing; Fig. 1, steps 3 and 4), while deacylation of misaminoacylated tRNAs occurs at a separate domain dedicated for post-transfer editing (step 5).

isoleucyl-tRNA synthetase (IleRS) is a well-studied enzyme, responsible for charging $tRNA^{Ile}$ with Ile. It bears high structural resemblance with leucyl- (LeuRS) and valyl-tRNA synthetase (ValRS). Accordingly, these three enzymes (I/L/VRSs) are thus classified in the Ia subgroup [10] and likely diverged from one common ancestor. Among other features, these three enzymes possess a domain dedicated for post-transfer editing—insertion in the so-called connective peptide 1 (CP1) protodomain that is present in all class I aaRSs.

IleRS has been long known to misrecognize Val [11] and uses both tRNA-dependent pre-transfer editing of Val-AMP within the synthetic site (Fig. 1, path 4) [12] and deacylation of $Val\text{-}tRNA^{Ile}$ at the post-transfer editing domain (Fig. 1, path 5) [13,14] to clear the outcome of Val misrecognition. However, besides Val that is the well-established non-cognate substrate of IleRS, norvaline (Nva) also acts as aminoacylation surrogate of Ile. Nva is a non-canonical amino acid that is a side-product of leucine biosynthesis [15]. Pezo *et al.* [16] demonstrated that Nva incorporation into cellular proteins is prevented by IleRS post-transfer editing, and that in the absence of IleRS editing, Nva is toxic. However, the mechanistic basis of Nva recognition, aminoacylation and editing by IleRS remains unknown. Furthermore, Nva and Val represent an interesting pair for comparison of mistranslation effects *in vitro* and *in vivo* by a single aaRS (herein IleRS), something that has not yet been addressed. Val is ever-present and typically available at high concentration, for example, in *Escherichia coli* at around 4 mM [17]. On the other hand, Nva accumulates only under microaerobic growth up to approximately 1 mM concentration [5]. Having the same molecular mass, Val and Nva differ only in the structure of their side chains—Val being β-branched and Nva linear. Thus, these two amino acids may incur different effects on protein folding and stability when substituting Ile, with the linear Nva being potentially more deleterious [18,19]. Hence, a particularly interesting question that remains unanswered is whether Nva misincorporation into proteins is more deleterious compared to Val, and conversely, if and how IleRS differs in its discrimination against Nva compared to Val (in either the synthetic and/or the editing pathways).

With this in mind, we set to examine Nva as a mimic of Ile in aminoacylation and compare it to the previously studied Val. We examined aaRS kinetics *in vitro*, and also misincorporation of Nva and Val *in vivo*. *In vitro*, we found that Nva and Val are equally acceptable non-cognate substrates in the synthetic reaction of IleRS, both discriminated by 200-fold relative to Ile. We found, however, that editing of $Nva\text{-}tRNA^{Ile}$ is more efficient. Why did IleRS evolve superior editing against a sporadically present non-cognate amino acid? To answer this question, we used a strain with inactivated IleRS editing domain to test the effect of Nva and Val mistranslation *in vivo* and to correlate it with their misincorporation into *E. coli* proteins. This analysis showed that proteome-wide substitution of Ile with Nva occurred to a similar extent and at the same Ile positions as substitution of Ile with Val. Nonetheless, Nva misincoproration incurred higher toxicity. Surprisingly, we found that ValRS efficiently edits $Nva\text{-}tRNA^{Val}$, although it discriminates sufficiently well against Nva at the synthetic step. Taken together with our recent finding that Nva is a prime target of the LeuRS editing domain [20], our results raise some

intriguing hypotheses regarding the evolutionary history of IleRS, ValRS and LeuRS, and participation of Nva in primordial proteins.

Results

Our kinetic analysis was designed to address two questions: (i) Does IleRS display different misincorporation rates of sporadically present non-proteinogenic Nva relative to ever-present Val? and (ii) If so, which individual step(s) in the synthetic and editing reactions mediates the different aminoacylation propensities of IleRS toward Nva and Val? The first question was addressed through a steady-state analysis of the overall rates of Nva-tRNA^{Ile} formation and editing. This approach examines multiple turnover conditions, largely the manner by which enzymes operate in cells, thus providing the basis for comparison of *in vitro* and *in vivo* data. However, this analysis cannot address the mechanistic issues posed under the second question. Therefore, to unveil details of the mechanism by which IleRS discriminates against Nva and Val, the individual synthetic and editing steps were analyzed in isolation, using either steady-state or single-turnover conditions as appropriate.

IleRS exhibits lower misaminoacylation rate with Nva than with Val

ATP is used stoichiometrically (one ATP per amino acid) in aminoacylation. However, enhanced ATP consumption is observed in the presence of non-cognate amino acids due to active editing that results in futile cycles of the synthetic and hydrolytic reactions (Fig. 1). Therefore, aaRS editing can be detected as an increase in [^{32}P]AMP formation [21] in the presence of non-cognate amino acids. Here we applied our recently developed assay [12,22] that follows AMP formation (k_{AMP}) and in a parallel reaction, under the very same conditions, formation of misaminoacylated tRNA ($k_{aa\text{-}tRNA}$) using [^{32}P] tRNA. This approach also provides the AMP/aa-tRNA ratio that reflects the efficiency of editing, that is, the number of ATP consumed per accumulated misaminoacylated tRNA.

We found that, in the presence of 100 mM Nva, IleRS accumulated trace amounts of Nva-tRNA^{Ile}, while AMP accumulation was substantial under the identical steady-state conditions (k_{AMP} = 2.64 s^{-1}, Table 1). This demonstrates that Nva-tRNA^{Ile} accumulation is prevented by pre- and/or post-transfer editing (indistinguishable by this approach). The AMP/Nva-tRNA^{Ile} ratio (≥2000, Table 1) reports approximately 2000 error-correction cycles per each erroneously released Nva-tRNA^{Ile}, thus indicating efficient editing of Nva. For comparison, the ratio obtained with the cognate amino acid gives an AMP/Ile-tRNA^{Ile} ratio of 1.5 [12].

Surprisingly, this AMP/Nva-tRNA^{Ile} ratio is substantially higher that the previously measured AMP/Val-tRNA^{Ile} ([12]; Table 1). The higher AMP/Nva-tRNA^{Ile} ratio results from both higher k_{AMP} (2.5-fold) and lower $k_{Nva\text{-}tRNA}$ (~50-fold). As a consequence, IleRS accumulates Val-tRNA^{Ile} to a significantly higher extent than Nva-tRNA^{Ile}. However, the observed aminoacylation could also originate from cognate aminoacylation of Ile that might be present at trace amounts in the Val sample. The overall amount of AA-tRNA observed with 20 mM Val was 6 μM, and thus, if ascribed to Ile contamination, this level corresponds to 0.03%. Thus, a 10-fold lower Val concentration should yield a total level of AA-tRNA of 0.6 μM, and accordingly a different AMP/AA-tRNA^{Ile} ratio. However, using 2 mM Val, we aminoacylated more than 3 μM of tRNA and obtained the same AMP/Val-tRNA^{Ile} ratio (Table 1) as with 20 mM Val, indicating that the formation of Val-tRNA^{Ile} is indeed being monitored. Furthermore, the formation

Table 1. Steady-state rate constants for AMP and AA-tRNA^{Ile} formation[a]

	k_{AMP} (s^{-1})	$k_{AA\text{-}tRNA}$ (s^{-1})	$k_{AMP}/k_{AA\text{-}tRNA}$	k_{ed}[b] = $k_{AMP} - k_{Nva\text{-}tRNA}$ (s^{-1})
WT IleRS + Nva (100 mM)	2.54 ± 0.08	≤10^{-3}[c]	≥2035	2.54
WT IleRS + Nva (2 mM)	0.25 ± 0.06	N.D.[d]		
D342A/T243R IleRS[e] + Nva (100 mM)	1.63 ± 0.07	0.56 ± 0.02	2.9	1.07
WT IleRS + Val (20 mM)[f]	0.97 ± 0.02	0.06 ± 0.003	16	0.91
WT IleRS + Val (2 mM)	0.30 ± 0.07	0.015 ± 0.002	19	0.29
D342A IleRS[g] + Val (20 mM)[f]	0.40 ± 0.006	0.13 ± 0.006	3.1[h]	0.28

The values represent the best fit ± SE from ≥3 independent experiments.

[a] AMP formation and tRNA misaminoacylation were followed in parallel reactions under the same conditions.

[b] k_{ed} represents formation of AMP solely from editing.

[c] Nva-tRNA^{Ile} accumulated to trace amounts. In some experiments, we were not able to trace it. We thus estimate the aminoacylation rate to be ≤0.001. This brings some uncertainty in the comparisons that use this value.

[d] Not determined as Nva-tRNA^{Ile} could not be traced under these conditions.

[e] IleRS variant deprived of post-transfer editing of Nva-tRNA^{Ile} (see Table 3) and Val-tRNA^{Ile} ([23]).

[f] Data taken from Ref. [12].

[g] IleRS variant deprived of post-transfer editing of Val-tRNA^{Ile} ([14]).

[h] The AMP/Val-tRNA^{Ile} ratio of 2.8 was measured for the D342A/T243R mutant under the same conditions.

of Nva-tRNA^{Ile} could not be traced in the presence of 2 mM Nva in agreement with the observation of higher editing rates of Nva-tRNA^{Ile}. Ideally, the accumulation of AA-tRNA should be compared under the same concentration of Val and Nva. However, to observe trace amounts of Nva-tRNA^{Ile}, the concentration of Nva had to be raised up to 100 mM, while for Val, the concentration could not be raised above 20 mM due to the risk of Ile contamination. Nonetheless, this comparison indicates that IleRS accumulates Val-tRNA^{Ile} at higher rate than Nva-tRNA^{Ile} (0.06 *versus* $\leq 10^{-3}$ s^{-1}) even when Nva is present at higher concentration than Val.

Because the measured overall rates may be directed by different individual steps in the reaction pathways, we next isolated and kinetically characterized individual steps in the synthetic and editing reactions of IleRS to delineate the mechanism by which IleRS rejects Nva more efficiently than Val.

Nva and Val are equally activated by IleRS

Activation of Nva was assessed using the standard ATP-PPi exchange assay (Table 2). Nva was activated with a similar k_{cat} as the cognate Ile (41 s^{-1} *versus* 55 s^{-1}), while its K_M was higher by 200-fold (0.82 mM *versus* 0.0046 mM). The discrimination factor for Nva (defined as [k_{cat}/K_M (Ile)]/[k_{cat}/K_M (Nva)]) was thus 239, indicating that Nva can be readily activated by IleRS. These kinetic constants are highly similar to the constants obtained previously for Val (Table 2, [11]).

Recognition of Ile in the synthetic site of IleRS is mediated by tRNA, which increases the K_M for Ile by 10-fold (measured in the presence of aminoacylation inactive tRNA analogue) [24]. The K_M for Nva also increased by the same 10-fold (Table 2). Thus, as previously seen with Val [14], tRNA binding does not influence discrimination of Nva. Overall, Nva and Val are activated with similar efficiency, which is in both cases higher than the overall error of protein synthesis (average error frequency 10^{-3}) [1], suggesting that IleRS editing plays a role with both these amino acids.

Table 2. Kinetic parameters for Nva activation by IleRS and ValRS[a]

	K_M (mM)	k_{cat} (s^{-1})	k_{cat}/K_M (s^{-1} mM^{-1})	Discrimination factor[b]
IleRS				
Ile[c]	0.0046 ± 0.0005	55 ± 9	11,956	
Nva	0.82 ± 0.07	41 ± 1	50	239
Val[c]	0.47 ± 0.03	35 ± 6	75	159
IleRS + tRNA$^{Ile}_{ox}$[d]				
Ile[e]	0.081 ± 0.006	37 ± 1	457	
Nva	7.9 ± 0.5	25 ± 3	3.2	143
Val[e]	11 ± 2	31 ± 2	2.8	163
ValRS				
Val[c]	0.048 ± 0.008	64 ± 2	1333	
Nva	14 ± 2	4.3 ± 0.2	0.3	4443

The values represent the best fit value ± SE of at least three independent experiments.
[a] Activation is followed by ATP-PP$_i$ exchange assay.
[b] Discrimination factor is defined as [k_{cat}/K_M (cognate aa)]/[k_{cat}/K_M (non-cognate aa)].
[c] Data taken from Ref. [23].
[d] ATP-PP$_i$ was measured in the presence of aminoacylation inactive tRNA$^{Ile}_{ox}$, an tRNA^{Ile} analogue having vicinal diols at the terminal ribose oxidized to dialdehydes
[e] Data taken from Ref. [14].

Nva is rapidly transferred to tRNA^{Ile}

Next, we tested the second step of aminoacylation—the transfer of the norvalyl moiety to tRNA. Because WT IleRS efficiently hydrolyses Nva-tRNA^{Ile}, an IleRS mutant that is inactive in post-transfer editing was used (T243R/D342A IleRS; see below). The editing-deficient IleRS mutant was preincubated with Nva and ATP to promote *in situ* formation of the IleRS:Nva-AMP complex and subsequently mixed with a limiting amount of [^{32}P]tRNA^{Ile} using a rapid chemical quench. Time-dependent Nva-[^{32}P]tRNA^{Ile} formation fits well a single exponential with a k_{trans} of 10.6 s^{-1} (Fig. 2). This transfer rate appears faster than the transfer rate for cognate Ile (2.2 s^{-1}, Fig. 2) and Val (0.8 s^{-1}, Fig. 2 and [14]). Thus, Nva is a good surrogate of Ile in both aminoacylation steps, similar or even to some extent better than Val.

IleRS synthetic site hydrolyzes Nva-AMP through tRNA-dependent pre-transfer editing

The steady-state assays showed that Nva is edited by IleRS—apparently even better that Val (Table 1). However, these assays cannot indicate whether Nva is edited through pre- and/or post-transfer editing.

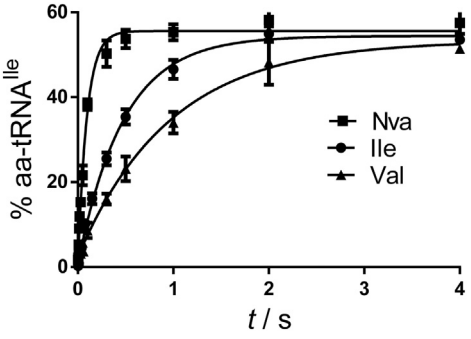

Fig. 2. Single-turnover transfer of Nva, Ile and Val to tRNA^{Ile} by IleRS. To measure transfer rates, post-transfer editing must be inactivated, and hence, an IleRS variant carrying two mutations in the editing domain was applied (IleRS-T243R/D342A). Time-points fit a single exponential with a rate constant of k_{trans} (Ile) = 2.2 ± 0.1 s^{-1}, k_{trans} (Nva) = 10.6 ± 0.9 s^{-1} and k_{trans} (Val) = 0.87 ± 0.01 s^{-1}. Error bars correspond to the SE from three independent experiments.

Among I/L/VRSs, IleRS appears unique in using tRNA-*dependent* pre-transfer editing, a pathway that occurs in the synthetic site (Fig. 1, path 4). This pathway was demonstrated [11] and kinetically analyzed only for erroneously activated Val [12]. To study tRNA-dependent pre-transfer editing, a mutant lacking post-transfer editing must be used (T243R/D342A IleRS, see below). However, even with the post-transfer editing-deficient mutant, one cycle of tRNA misaminacylation occurs, thus contributing to AMP formation in parallel with pre-transfer editing. To isolate these two contributions to AMP formation, we followed [^{32}P]AMP formation (k_{AMP}) in parallel with misaminoacylation of [^{32}P]tRNA ($k_{aa\text{-}tRNA}$) as described above for WT IleRS. The rate of pre-transfer editing (k_{ed}) was then derived by subtracting $k_{aa\text{-}tRNA}$ (representing AMP that originates from misaminoacylation) from the k_{AMP}.

We found that T243R/D342A IleRS accumulated [^{32}P]AMP in the presence of Nva and tRNA with a rate constant of $k_{AMP} = 1.63\ s^{-1}$, while AMP accumulation arising solely from misaminoacylation proceeded with a rate constant of $0.56\ s^{-1}$ (Table 1). The AMP/Nva-tRNA^{Ile} ratio of 3 thus indicates pre-transfer editing with the rate constant of $1.07\ s^{-1}$. Note that the AMP/Nva-tRNA^{Ile} ratio is significantly lower for T243R/D342A than for the WT—the latter has both pre- and post-transfer editing, while the former has only pre-transfer editing and hence significantly misaminoacylates tRNA with Nva ($k_{Nva\text{-}tRNA} = 0.56\ s^{-1}$, Table 1). The rate of tRNA-*independent* editing was determined separately by following increase in AMP formation in the absence of tRNA ($k_{ed\text{-}tRNA} = 0.086\ s^{-1}$) suggesting a minor contribution compared to tRNA-dependent pre-transfer editing ($1.07\ s^{-1}$).

The above data are analogous to the previously acquired data with Val (Table 1) showing that erroneously activated Nva and Val are removed by IleRS pre-transfer editing with similar efficiency (i.e., with the same AMP/aa-tRNA ratios). Data for Val ([12]) were measured with D342A IleRS that is unable to hydrolyze Val-tRNA^{Ile}, while herein, we present Nva data acquired with the T243R/D342A mutant that is inactive in both Val- and Nva-tRNA^{Ile} hydrolyses. To eliminate the possibility that different mutations in the editing domain result in different kinetics, we measured the AMP/Val-tRNA^{Ile} ratio for T243R/D342A and found it to be the same as for D342A (Table 1). Finally, when IleRSAla10 (the mutant inactivated in post-transfer editing, see below) was used, both the rates and the AMP/AA-tRNA ratios for Nva and Val were highly similar (Table S1). Comparison of the k_{ed} values for the post-transfer editing-deficient mutants to those of WT IleRS show that with both Nva (this study) and Val [12], tRNA-dependent pre-transfer-editing is a minor pathway compared to post-transfer editing. Altogether, our kinetic analysis supports a view that tRNA-dependent pre-transfer editing is an inherent IleRS activity and not a specific solution evolved for a particular amino acid.

IleRS post-transfer editing is better optimized for elimination of Nva-tRNA^{Ile}

Next, we tested IleRS post-transfer editing, the main editing pathway localized at the editing domain. Product release determines the steady-state rate of post-transfer editing [22], thus demanding single-turnover conditions. We followed the rate of deacylation of preformed Nva-[^{32}P]tRNA^{Ile} using rapid chemical quench in the presence of an excess of IleRS. The decrease in the percentage of Nva-tRNA^{Ile} fits a single exponential with a rate constant of $85\ s^{-1}$ (Table 3). The rate of deacylation of Nva-tRNA^{Ile} is 2-fold faster than the rate of Val-tRNA^{Ile} hydrolysis ($k_{deacyl} = 49\ s^{-1}$, Table 3). This is in agreement with the steady-state data showing better editing of Nva than Val (higher AMP/aa-tRNA ratio).

We next set to explore inactivation of Nva-tRNA^{Ile} deacylation. Mutation of the highly conserved Asp 342 led to a 4500-fold drop in the deacylation rate indicating that Asp342 is crucial for anchoring Val-tRNA^{Ile} for hydrolysis [25]. However, we found that the D342A mutation decreased Nva-tRNA^{Ile} deacylation by only 50-fold ($k_{deacyl} = 1.6\ s^{-1}$, Table 3). A substantial loss of post-transfer editing of Nva-tRNA^{Ile} was accomplished only with a second mutation that targets the interaction with the tRNA terminal ribose (Thr243Arg) [23,26]. Hence, T243R/D342A IleRS displayed about 10^4-fold drop in the rate of Nva-tRNA^{Ile} hydrolysis relative to WT IleRS ($k_{deacyl} = 0.0046\ s^{-1}$; Table 3). This indicates that the IleRS editing site establishes more anchoring contacts with Nva- than with Val-tRNA^{Ile}, and thus, hydrolysis of Nva-tRNA^{Ile} is less sensitive to inactivating mutations.

Table 3. Single-turnover rate constants for hydrolysis of aminoacyl-tRNAs[a]

		k_{deacyl} (s^{-1})
WT IleRS	Nva-tRNA^{Ile}	85 ± 10
WT IleRS	Val-tRNA^{Ile}	49 ± 6
D342A IleRS	Nva-tRNA^{Ile}	1.6 ± 0.1
D342A/T243R IleRS	Nva-tRNA^{Ile}	0.0046 ± 0.0003
WT ValRS	Nva-tRNA^{Val}	450 ± 131 s^{-1}[b]
WT ValRS	Thr-tRNA^{Val}	438 ± 47

The values represent the best fit value ± SE of at least three independent experiments.

[a] The enzymes concentrations were as follow: 10 μM WT IleRS, 30 μM D342A IleRS, 30 μM D342A/T243R IleRS and 30 μM ValRS. In all reactions, the enzyme concentration was ≥20-fold higher than AA-RNA.

[b] Nva-tRNA^{Val} hydrolysis showed biphasic behavior with about 30% of Nva-tRNA^{Val} hydrolyzed with the rate constant of 450 ± 131 s^{-1}, while the remaining was hydrolyzed at 0.13 ± 0.3 s^{-1}.

ValRS also rapidly hydrolyzes Nva-tRNA^{Val} at its editing domain

IleRS's closest homologs are LeuRS and ValRS—these three enzymes share common ancestry of both the synthetase and the post-transfer editing domains. Similar to IleRS, LeuRS rapidly deacylates Nva-tRNA^{Leu} (k_{deacyl} = 310 s^{-1}) [22]. This prompted us to explore how ValRS discriminates against Nva. ValRS activated Nva with 300-fold higher K_M and 15-fold lower k_{cat} than cognate valine. This discrimination factor of 4443 (compared to 239 for Nva and IleRS; Table 2) is sufficiently high to support high fidelity protein synthesis. It thus appears that ValRS would not require editing of Nva-tRNA^{Val}.

We tested the rate of hydrolysis of Nva-[^{32}P]tRNA^{Val} by ValRS under single-turnover conditions as described above for IleRS, and found it to be surprisingly high (Table 3). Notably, a similar rate was obtained for hydrolysis threonyl-tRNA^{Val} (Thr-tRNA^{Val}, Table 3), in agreement with Thr being poorly discriminated by ValRS synthetic site (discrimination factor of 270) [23]. Thus, despite the sufficiently high discrimination of Nva by its synthetic site, ValRS still rapidly hydrolyses Nva-tRNA^{Val} at its editing domain. It appears, therefore, that post-transfer editing of Nva is a common feature of all three extant I/L/VRSs regardless if needed (IleRS and LeuRS) or not (ValRS), suggesting that the important evolutionary pressure for acquisition of the editing domain was to prevent infiltration of Nva into proteins.

In vivo Nva exhibits higher toxicity than Val when incorporated at Ile protein sites

Taken together, *in vitro* kinetics revealed that Nva is better edited by IleRS, suggesting that Ile-to-Nva mistranslation could be more deleterious than Ile-to-Val. To compare the effects of mistranslation *in vivo*, we used a previously described *E. coli* strain relying on an editing-deficient IleRS [16]. In that strain (IleRS ED$^-$, PS7066) wild-type (WT) chromosomal IleRS was replaced with a mutant in which the conserved threonine-rich peptide (T241–N250) in the editing domain was substituted with 10 consecutive Ala residues (IleRSAla10). As expected, this strain exhibits growth defects when challenged with Nva or Val [16]. Our attempts to create an *E. coli* strain with genomic double mutant IleRS used for *in vitro* kinetics (T243R/D342A) were not successful. However, we confirmed *in vitro* that IleRSAla10 is, like T243R/D342A IleRS, inactive in post-transfer editing (k_{deacyl} for Nva- and Val-tRNA^{Ile} were 0.0008 ± 0.0002 s^{-1} and 0.0007 ± 0.0002 s^{-1}, respectively) and equivalently discriminates Nva and Val in activation (Supplementary Table S2). Determination of AMP/aa-tRNA ratios (Supplementary Table S1) revealed also similar pre-transfer editing of Nva and Val by IleRSAla10. Thus, as is the case with WT IleRS, IleRSAla10 utilized Nva and Val equally well in the synthetic and pre-transfer editing reactions, demonstrating that strain IleRS ED$^-$ is suitable for comparing Nva and Val mistranslation *in vivo*.

The effect of mistranslation was measured by challenging the growth of strain IleRS ED$^-$ by addition of either Nva or Val (Supplementary Fig. S1). Excess of Val produces Ile pseudoauxotrophy in strains derived from *E. coli* K12 [15]; hence, the growth conditions included Ile, Leu and Val, each at 100 μM concentration. The analysis revealed that in 1-mM range, Nva inhibited the growth of IleRS ED$^-$ significantly more than Val. However, at higher concentrations, Nva and Val had similar toxic effect that resulted in complete growth inhibition when each was present at ≥10 mM (Fig. 3A). Thus, at this point, mistranslation with either Nva or Val becomes highly toxic. Albeit the IC_{50} values were similar (1.6 ± 0.1 mM for Nva and 1.98 ± 0.04 mM for Val), the difference is reproducible and statistically significant (p = 0.018). Furthermore, the IC_{50} values appear to underestimate the difference in Nva *versus* Val toxicity. The growth of MG1655 was insensitive to added Nva or Val (Fig. 3A), confirming that the effect in strain IleRS ED$^-$ is primarily due to mistranslation.

Next, we tested viability of IleRS ED$^-$ strain during prolonged growth supplemented with 2 mM Nva or 2 mM Val. We found that cells survival significantly differs after 24 h of growth; the number of colony-forming units (CFU) was 4-fold lower in the presence of Nva compared to Val (Fig. 3B). Under the same conditions, the WT strain did not show a decrease in viability (Fig. 3B). Taken together, our data indicate that Nva mistranslation inhibits *E. coli* growth to a significantly larger extent compared to Val, thus providing rationale for our findings that Nva is a preferred target of the IleRS editing.

Nva and Val are incorporated with equal frequencies into the proteome

Nva exhibited higher toxicity than Val, indicating that Nva misincorporation at Ile positions may incur higher penalty to protein structures and/or functions. Val and Ile are both beta-branched, while Nva linear side chain may be more destabilizing. On the other hand, it is also possible that *in vivo*, Val is better discriminated than Nva, by IleRS, or *via* other mechanisms, thus making Val misincorporation less frequent and thereby less toxic. To compare the levels of misincorporation, we performed mass spectrometry (MS)-based proteome analyses of IleRS ED$^-$ strain upon adding exogenous Nva or Val. The parental strain MG1655 with genomic WT IleRS was used as a control. Both strains were grown to mid-exponential phase in the presence of 0.5 or

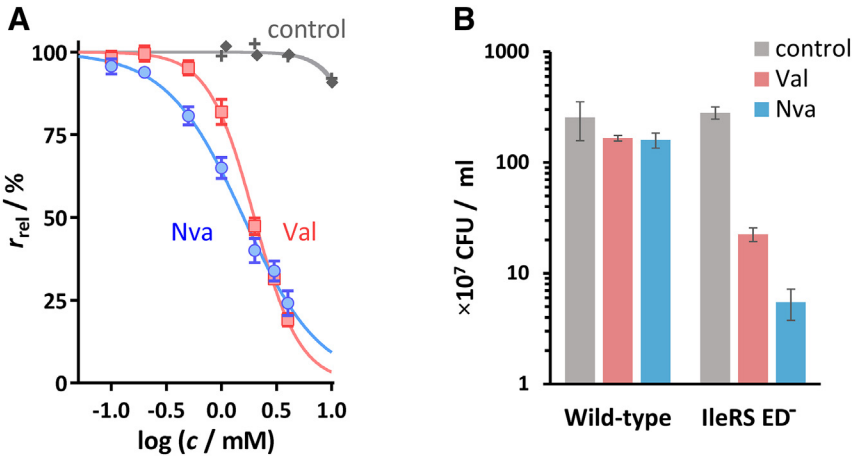

Fig. 3. *In vivo* toxicity of Nva and Val in the absence of IleRS post-transfer editing. (A) Growth inhibition. The growth rates of an *E. coli* strain deprived of IleRS post-transfer editing (IleRS ED$^-$) were monitored in enriched M9 supplemented with either Val or Nva (0.1–10 mM, Supplementary Fig. S1). The growth rate constants were extracted by fitting to the exponential equation (see Materials and Methods). The IC_{50} values derived from fitting the growth rate constants to the logistic equation were 1.6 ± 0.1 mM (Nva) and 1.98 ± 0.04 mM (Val). The IC_{50} values are given as arithmetic mean ± SE of four independent determinations. The paired *t* test (two-tailed) *p* value was 0.018, indicating that the IC_{50} values for Nva and Val differ significantly. WT strain MG1655 (a control with IleRS post-transfer editing) did not show growth inhibition under the same conditions. The figure shows the best curve fit to the averaged growth rate constants for Nva and Val; error bars correspond to SEs (n = 4). (B) Cell viability. IleRS ED$^-$ was grown in enriched M9 supplemented with either 2 mM Nva or 2 mM Val. The number of colony-forming units (CFU/ml) after 24 h growth was (5.5 ± 1.7) × 10^7 (Nva) and (22.5 ± 3.2) × 10^7 (Val). The control was done in enriched M9 without exogenously added Nva or Val ((282 ± 35) × 10^7). WT strain MG1655 did not show a decrease in viability in enriched M9 supplemented with either 2 mM Nva or 2 mM Val. Error bars correspond to SD from three biological replicates.

2 mM of either Nva or Val (Fig. 4A). Upon lysis, the total proteome was analyzed by high-resolution liquid chromatography–tandem MS (LC–MS/MS).

Proteome-wide MS analysis of IleRS ED$^-$ indicated that given the same concentrations of exogenously added Nva or Val, Ile positions were mistranslated at similar frequencies (Fig. 4B). Thus, in agreement with *in vitro* results, in the absence of post-transfer editing, Nva and Val appeared as similar competitors of Ile in aminoacylation *in vivo*. The frequencies of Ile mistranslation at 0.5 mM Nva and Val were 6% and 8%, respectively. When challenged with 2 mM Nva or Val, misincorporation frequencies increased to 14% for Nva and 20% for Val (Fig. 4B, Supplementary Table S3). Nva and Val misincorporations at Leu positions (control for the accuracy of misincorporation assignment, see M&M) was negligible, as expected (Supplementary Table S4). Owing to its active IleRS editing, WT MG1655 exhibited significantly lower Ile mistranslation under the same conditions (Fig. 4B). Because Nva accumulates only under microaerobic growth [5,7], misincorporations observed with supplemented Val were all assigned to Val rather than Nva. Lower mistranslation at Leu positions in MG1655 when growth was supplemented with Val compared to Nva (Supplementary Table S4) confirmed that Nva does not endogenously accumulate under the applied conditions (LeuRS can mistranslate Nva to some extent but not Val [7]). Endogenously synthesized Val and Val added to all media (100 μM) could also compete with the supplemented Nva. Therefore, a control experiment was performed wherein the IleRS ED$^-$ strain was grown in a medium supplemented only with 100 μM Ile, Leu and Val. Under these conditions, mistranslation at Ile positions was 0.3% (Fig. 4B, Supplementary Table S3) indicating a very low background frequency of Ile-to-Val mistranslation in our experimental setup. Thus, in IleRS ED$^-$ grown in the presence of Nva, misincoporation arises from Ile-to-Nva substitutions. Taken together, our data revealed that similar frequencies of Nva or Val misincorporation induced the noteworthy difference in cellular toxicity: cells with 14% Ile-to-Nva mistranslation exhibited 4-fold lower viability compared to cells with 19% Ile-to-Val misincorporation.

Nva and Val misincorporate at the same Ile positions and proteins

Misincorporation of Nva at equal or even lower rate compared to Val inflicted higher growth inhibition. A simple explanation could be that Nva and Val are misincorporated into different positions and/or different proteins. To address this, we further analyzed the MS data from the strain IleRS ED$^-$ grown in the presence of exogenously added Nva or Val. The likelihood of detecting misincorporation at a given Ile

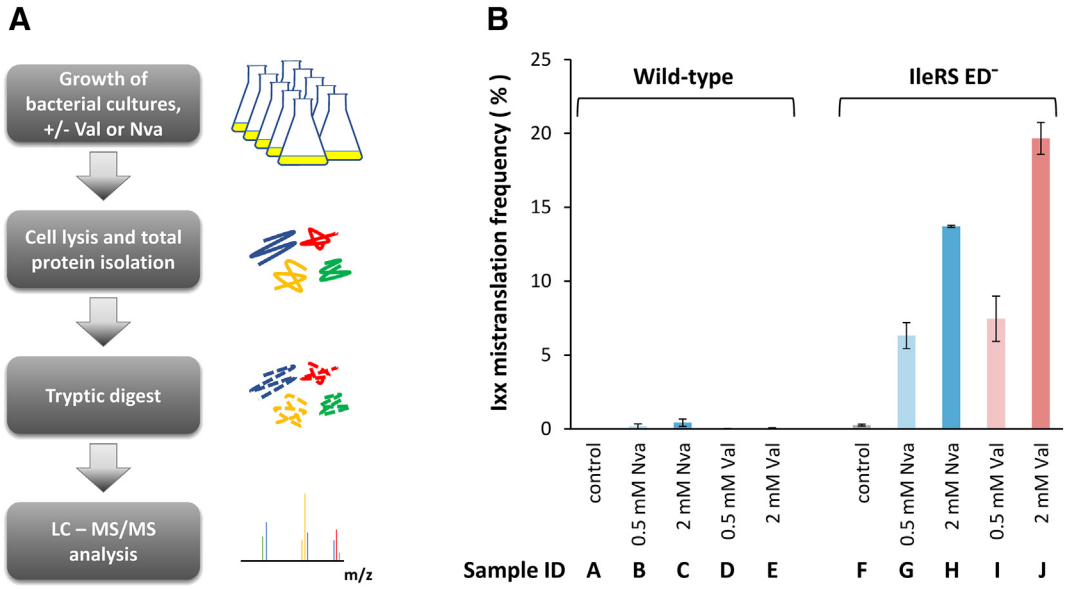

Fig. 4. Nva and Val misincorporation at Ile positions of *E. coli* proteins in the absence of IleRS post-transfer editing. (A) Experimental workflow. WT strain MG1655 and its strain deprived of IleRS post-transfer editing (IleRS ED⁻) were grown in enriched M9 with or without exogenously added Val or Nva (0.5 mM or 2 mM). The proteomes were isolated and digested, and amino acid misicorporation was analyzed by LC–MS/MS at high resolution. (B) MS/MS analysis. The frequency of Ile-to-Nva or Ile-to-Val substitutions (Ixx) was determined by counting of MS/MS spectra that corresponded to correctly translated peptides (with Ile) *versus* mistranslated ones (with either Nva or Val). To calculate the frequency of mistranslation, the total number of Ixx substitutions identified in all Ixx-containing MS/MS spectra was divided by the total number of expected Ile positions in all analyzed peptides (Ixx + Ile). Error bars correspond to SD from three biological replicates. The control represents mistranslation observed during growth in enriched M9 only.

position is proportional to the frequency by which this position is sampled. Thus, to reduce sampling bias, we examined only peptides observed at least 4 times (Supplementary Fig. S2) and in all analyzed conditions (Supplementary Table S5). The analysis revealed a high degree of overlap between the unique Ile positions mistranslated under different error-prone conditions (Fig. 5). The vast majority of Ile sites that were observed mistranslated at low exogenous Nva and Val concentrations (0.5 mM) are also mistranslated at higher concentrations (2 mM) (93% and 94%, respectively; Fig. 5A and B). Out of the 1178 Ile positions measured, 734 are identified as mistranslated by both Nva and Val under at least one condition (0.5 or 2 mM), and the overlapping positions comprise 91% and 81% of all mistranslated sites with Nva and Val, respectively (Fig. 5C). This high overlap and the high percentage of mistranslated Ile positions (66% and 74% for Nva and Val, Supplementary Table S5) indicated that

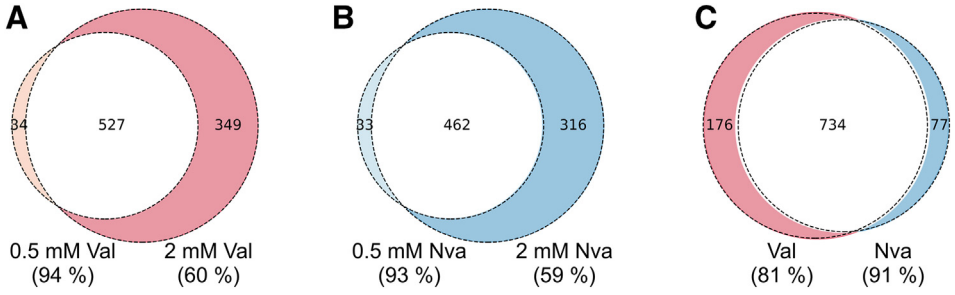

Fig. 5. Ile positions that are mistranslated with Nva and Val overlap. Venn diagrams depicting the overlap between the unique Ile positions (defined by the location of the Ile residues in the primary sequences of *E. coli* proteins) identified as mistranslated at least once in IleRS ED⁻ strain. The analysis includes positions identified in peptides that were measured ≥4 times (Supplementary Fig. S2) under all conditions (samples F–J, Fig. 4). (A) Comparison of Ile positions identified in 0.5 and 2 mM exogenously added Val. (B) Likewise for 0.5 and 2 mM exogenously added Nva. (C) Comparison of Ile positions identified as mistranslated by *both* Nva and Val under at least one condition (0.5 or 2 mM, samples G *versus* I, or H *versus* J; Fig. 4). The percentages of overlapping positions are shown in parenthesis.

misincorporation is random and is likely to occur at most Ile positions given enough sampling. Indeed, we observed overlap of mistranslated Ile positions approaching 100% using higher sampling threshold (Supplementary Fig. S3). Thus, based on the analysis of proteins that are more easily detected in cells, Nva and Val seem to be misincorporated within the same positions and proteins, suggesting that Nva is more toxic because its misincoporation imposes more damage compared to Val.

Discussion

Nva and Val present an interesting comparison for exploring mistranslation effects by a single aaRS. Val is an ever-present proteinogenic amino acid, while Nva accumulates only under microaerobic growth [5] and is not coded for protein synthesis. Having the same mass, Nva and Val differ only in the structure of their side chains: Val has a beta-branched side chain, while Nva has a linear. They can both compete with Ile in aminoacylation and are substrates of IleRS editing. However, opposed to Val whose recognition by IleRS was well studied [11,12,14,23], the mechanism of participation of Nva in IleRS reactions remains unknown. Here, we performed an *in vitro* analysis of aminoacylation and editing of Nva and compared it with the previously studied Val. We also compared the degree and effects of misincorporation of both Nva and Val *in vivo*.

IleRS generates aminoacylated tRNAs *via* a multiple step cycle that includes several editing steps (Fig. 1). Our data indicate that Nva and Val are similarly treated by IleRS in both steps of aminoacylation—both being discriminated at the activation step with a 200-fold specificity relative to the cognate Ile (Table 2, Fig. 2). However, this value is far below the threshold of translational errors, thus indicating that editing plays an important role in IleRS with both Nva and Val. We further showed that, within its synthetic site, IleRS hydrolyses erroneously activated Nva and Val with similar efficiency *via* tRNA-dependent pre-transfer editing (Table 1; Fig. 1, path 4). Overall, Nva and Val are similarly treated in both the synthetic and editing reactions of the IleRS synthetic site. However, when the overall reaction cycle, which includes post-transfer editing, is examined, IleRS edits Nva substantially more efficiently than Val. Thus, through multiple turnovers, $tRNA^{Ile}$ misaminoacylated with Val accumulates at rate that is approximately 50-fold faster than with Nva (Table 1). Single-turnover kinetics accordingly revealed that the editing site mediates hydrolysis of Nva-$tRNA^{Ile}$ at 2-fold faster rate compared to Val-$tRNA^{Ile}$ (Table 3). The smaller difference measured in the single-turnover reaction compared to the multiple-turnover one indicates that some other additional steps in IleRS catalytic cycles differ between Nva and Val, most likely tRNA displacement and/or release.

Why does IleRS exhibit superior editing against Nva? To this end, we tested the consequences of misincorporation of Nva and Val *in vivo* using an *E. coli* strain lacking the functional IleRS editing domain (herein named IleRS ED^{-}) [16]. Proteome MS/MS high-resolution analysis revealed that under these error-prone conditions, Nva and Val misincorporated with similar frequency (Fig. 4). Thus, both the *in vivo* and *in vitro* analyses indicated that in the absence of post-transfer editing, Nva and Val are equally good substrates of IleRS. Nonetheless, a similar level of misincorporation of Nva (14%) and Val (20%) into *E. coli* proteome (Fig. 4) resulted in about 4-fold higher toxicity with Nva (Fig. 3B). Higher toxicity with Nva occurs despite the fact that the proteins, and Ile positions within these proteins, that are mistranslated by Nva and Val overlap (Fig. 5). Overall, it appears that higher toxicity of Nva relates to the higher damage it inflicts on *E. coli* proteins. Higher damage is presumably a consequence of the higher conformational entropy associated with the linear side-chain of Nva compared to the beta-branched of Val, thus providing the rationale for IleRS editing being better tailored for elimination of Nva-$tRNA^{Ile}$.

On the evolutionary origin of Nva editing

What might be the evolutionary origin of editing against Nva? This cannot be conclusively established, yet we propose some ideas and hypotheses. IleRS shares common ancestry with the two other branched hydrophobic aaRSs—ValRS and LeuRS. We have recently shown that LeuRS efficiently misactivates Nva and hydrolyzes Nva-$tRNA^{Leu}$ rapidly at its editing domain [22]. ValRS, as shown here, discriminates against Nva well enough to support its overall fidelity of translation (4000-fold, Table 2). This suggests that ValRS has not been under evolutionary pressure to edit against Nva. Strikingly, however, ValRS hydrolyzed Nva-$tRNA^{Val}$ (Table 3), which presumably presents its latent activity. Latent activities typically comprise a vestige of an enzyme's ancestral function ([27]), thus supporting the view that editing of Nva-tRNA existed in the last common ancestor of I/L/VRSs, which likely preceded the last universal common ancestor (LUCA).

The idea that editing of Nva-tRNA was present in the last common ancestor of I/L/VRSs is in agreement with the view that Nva was present in the pre-LUCA environment. Nva is found in meteorites and accumulates to high degree in the Miller experiment that imitated the conditions of the early Earth atmosphere [28]. Both these findings were taken as indication of Nva ancient history [28,29]. That editing against Nva-tRNA likely existed in the last

common ancestor of I/L/VRSs provides an additional and independent indication for Nva ancient history.

Why is then Nva absent in the canonical amino acid alphabet? We hypothesize that Nva had participated in early translation but was later removed. Because Nva resembles Ile, Leu and also Val to an extent, it was presumably not efficiently discriminated by the early ancestor of I/L/VRSs, which comprised the class defining catalytic core only [30–32]. Furthermore, Nva was likely present at higher amounts than Val, Leu or Ile in the primordial conditions [28] (and may have been even explicitly synthesized [33]). This might have promoted aminoacylation and translation of Nva [34] to yield primordial "statistical proteins." However, an early ancestor of I/L/VRSs could have proofread aminoacyl-AMPs, although presumably to a limited extent. The discovery of Nva-AMP hydrolysis by IleRS (Table 1), LeuRS [22] and ValRS (data not shown) indicates that pre-transfer editing might had been indeed present in the I/L/VRSs ancestor. Furthermore, pre-transfer editing can still be traced in the synthetic domains of extant I/L/VRSs [12,22,23,35] and many other aaRSs [36–38]. However, pre-transfer editing does not prevent misaminoacylation of tRNA in contemporary aaRSs, suggesting that even if the primordial pre-transfer editing was physiologically meaningful, it was insufficient to ensure accurate translation. The urge for faster and more accurate translation likely presented the driving force for the attainment of the post-transfer editing domain (for detailed discussion, see Ref. [12]). We further hypothesize that the need to eliminate Nva from protein synthesis was an important driving force for the acquisition of the editing domain, and that the domain was acquired by the early ancestor of I/L/VRSs *prior* to its duplication and divergence to three specialized enzymes [39]. Replacement of the linear Nva, or other non-proteinogenic linear side-chain amino acids such as α-aminobutyrate, by branched hydrophobic amino acids, and takeover of precise translation instead of statistical incorporation of hydrophobic amino acids, were likely critical in enabling the evolution of larger, more complex proteins with better-defined 3D structures. The toxicity of Nva when replacing Leu [7] and the higher toxicity of Nva relative to Val (Fig. 3) lend support to this idea.

Materials and Methods

Enzymes and tRNAs

IleRS (WT, D342A and T243R/D342A mutants) and ValRS (WT and D286A mutant) enzymes from *E. coli* were overexpressed and purified by Ni-NTA chromatography as described [23]. ValRS enzymes were further purified from bound Val-AMP by a preparative aminoacylation in 100 mM Hepes (pH 7.5), 20 mM $MgCl_2$, 2 mM DTT and 0.1 mg/ml BSA followed by urea/NaCl treatment and Ni-NTA chromatography as described [22,40]. The gene for IleRSAla10, in which the editing domain peptide T241–N250 was substituted with 10 Ala residues, was cloned from genomic DNA of the strain PS7066 (see below). IleRSAla10 was overexpressed, purified by Ni-NTA chromatography as other IleRSs and subjected to size-exclusion chromatography on Superdex Increase 200 10/300 GL (GE Healthcare) column equilibrated in 1 M NaCl, 50 mM Hepes, 5 mM β-mercaptoethanol and 5% glycerol to remove co-purified tRNA.

$tRNA^{Ile}_{GAT}$ (with the the native $A^1{:}U^{72}$ replaced by $G^1{:}C^{72}$) and $tRNA^{Val}_{TAC}$ from *E. coli* were overexpressed and purified as described [23]. Plateau aminoacylation established that the purified samples have ~75% (for $tRNA^{Ile}$) and 80% (for $tRNA^{Val}$) aminoacylation active tRNAs. $tRNA^{Ile}_{ox}$, having terminal diols oxidized to dialdehydes, was produced by previously established protocol using $NaIO_4$ [14]. [^{32}P]$tRNA^{Ile}$ and [^{32}P]$tRNA^{Val}$ were prepared using tRNA nucleotidyltransferase and [α-^{32}P]ATP as previously described [23,41].

Preparation of misaminoacylated tRNAs

Misaminoacylated $tRNA^{Ile}$ and $tRNA^{Val}$ variants were prepared by mixing approximately 0.3 μM [^{32}P]tRNA, 1 μM deacylation defective D342A IleRS or D286A ValRS, 4 mM ATP, 0.004 U/μl IPPase, 2 μM non-labeled tRNA and 2 mM Nva, Val or Thr in 100 mM Hepes (pH 7.5), 20 mM $MgCl_2$, 2 mM DTT and 0.1 mg/ml BSA, followed by phenol extraction and gel-filtration purification [14]. Misaminoacylated tRNAs were renatured prior to use as described [40]. The used enzymes had negligible amount of bound aa-AMP.

Amino acid activation

Misactivation of Nva was followed by ATP-PPi exchange assay [40] at 37 °C in a buffer containing 100 mM Hepes (pH 7.5), 20 mM $MgCl_2$, 0.1 mg/ml BSA, 4 mM ATP, 1 mM [^{32}P]PP_i (0.2–0.4 μCi μmol^{-1}) and 2 mM DTT. IleRS was 25 nM, ValRS was 100 nM and Nva was varying from 0.1 to 10 × K_M. The effect of tRNA on the Nva misactivation was assessed in the presence of 10 μM 2′,3′-dialdehyde tRNA ($tRNA_{ox}$). Misactivations of Nva and Val by IleRSAla10 (50 nM) were performed under the same reaction conditions with the addition of 150 mM NH_4Cl.

Parallel formation of AMP and aa-$tRNA^{Ile}$

Formation of [^{32}P]AMP and aa-[^{32}P]tRNA was followed in parallel steady-state reactions as described in Ref. [40]. The reactions were followed at 37 °C in 100 mM Hepes (pH 7.5), 20 mM $MgCl_2$,

0.1 mg/ml BSA, 2 mM DTT, 0.004 U/μl IPPase, 200 μM ATP and 150 mM NH_4Cl (only in the reactions with IleRSAla10) containing either [α-^{32}P]ATP or [^{32}P]tRNA^{Ile}. WT IleRS was 20 nM and IleRSAla10 was 20 nM, Val was 75 mM (for IleRSAla 10) or 2 mM (IleRS) and Nva was 2 mM or 100 mM.

Single-turnover aminoacyl transfer step

Deacylation defective IleRS D342A/T243R (20 μM) was incubated with 10 mM ATP and 8 mM Ile, 80 mM Val or 100 mM Nva in a buffer containing 20 mM Hepes (pH 7.5), 10 mM $MgCl_2$, 0.008 U/μl IPPase, 100 μM EDTA, 150 mM NH_4Cl and 10 μg/ml BSA, for 10–30 min at 37 °C, to promote formation of the IleRS D342A/T243R:aa-AMP complex (no difference between these incubation times was observed, indicating that consumption of ATP due to tRNA-independent editing is not a factor). The single turnover reactions were then performed by mixing the equal volumes of the *in situ* formed complex with 2 μM [^{32}P]tRNA^{Ile} (in the same buffer) using rapid chemical quench (KinTek RQF-3) (detailed protocol in Ref. [40]). Time-courses fit to an exponential equation ($y = Y_0 + A \times (1 - e^{-k_{trans} \times t})$), where Y_0 is the y intercept, A is an amplitude, k_{trans} represents the apparent rate constant of the aminoacyl transfer step and t is time.

Single-turnover deacylation

Assays were performed at [enzyme] ≥ 20×[AA-tRNA], thus ensuring pseudo-first order conditions and saturation with respect to the bound AA-tRNA. The renatured Nva-[^{32}P]tRNA^{Ile} or Nva- or Thr-[^{32}P]tRNA^{Val} (200–500 nM) in 5 mM NaOAc (pH 4.5) and 20 mM $MgCl_2$ were mixed with the equal volume of 10 μM WT IleRS, 30 μM D342A IleRS, 30 μM D342A/T243R IleRS or 30 μM ValRS [in 100 mM Hepes (pH 7.5), 20 mM $MgCl_2$ and 2 mM DTT] using KinTek RQF-3 (detailed protocol in Ref. [40]). In case of IleRSAla10, the enzyme (4 μM final) was mixed with a limiting amount of Nva- or Val-[^{32}P]tRNA^{Ile} and the reactions were quenched by hand. Time-courses fit to an exponential equation ($y = Y_0 + A \times e^{-k_{deacyl} \times t}$) where Y_0 is the y intercept, A is the amplitude; k_{deacyl} represents the apparent deacylation rate constant and t is time.

Bacterial strains, growth media and conditions

WT *E. coli* strain MG1655 was obtained from The Coli Genetic Stock Center (Yale University). An *E. coli* strain deprived of IleRS post-transfer editing (PS7066, herein named IleRS ED$^-$) was kindly provided by P. Schimmel [16].

Standard growth conditions for testing mistranslation included M9 media enriched with Ile, Leu, Val each at 100 μM (herein named enriched M9). To assay mistranslation, the growth was supplemented with various concentrations of Nva or Val.

Determination of IC_{50} values

Overnight cultures of IleRS ED$^-$ strain (in the enriched M9) were used to inoculate (1:100) 4 ml of the enriched M9 media supplemented with Nva or Val (0.1–10 mM). The growth at 37 °C and 250 rpm was monitored using Ultrospec 10 (GE Healthcare Life Sciences). To extract the growth rate constants (r), OD_{600} collected during the log phase were fitted to exponential equation ($y = y_0 e^{rt}$). The IC_{50} values (inhibitory concentrations that decreased the growth rate constants by 50%) were calculated by fitting the r to equation $r = r_0/(1 + 10^{(a - x)b})$, where $x = \log(c/\text{mM})$ and a is $\log(IC_{50}/\text{mM})$.). The IC_{50} values for Val or Nva were independently determined four times. The IC_{50} values obtained from these individual measurements were averaged, and the IC_{50} values reported comprise the arithmetic mean ± SE. Statistical significance of the difference between the IC_{50} values for Val and Nva was tested by paired Student's t test (two-tailed) that gave a p value of 0.018 (p values <0.05 represent statistically significant differences). Alternatively, the input data (growth rates from the four independent experiments) were averaged, and the IC_{50} values were calculated by the non-linear regression from the averaged data points, with the residuals weighted by the standard deviation during fitting. This procedure yielded essentially identical IC_{50} values as the procedure described previously, with a comparable statistical confidence. The WT strain (MG1655) showed no appreciable growth inhibition in the given Val and Nva concentration range.

Cell viability test

Overnight cultures of WT and IleRS ED$^-$ strain were diluted 100-fold in the enriched M9 supplemented with 2 mM Val or Nva. The cultures were left at 37 °C and 250 rpm for 24 h, to reach stationary phase. Serial dilutions of the cultures were spread on the LB plates. After 16–24 h at 37 °C, colonies formed at appropriate dilutions were counted using OpenCFU 3.9.0 [42] to calculate colony-forming units per milliliter of the starting culture (CFU/ml). As a control, the strains were grown under the same conditions without the addition of 2 mM Val or Nva. In all cases, the bacterial cultures reached similar turbidity in stationary phase.

Proteome sample preparation for MS

The bacteria were grown at 37 °C in enriched M9. Mistranslation was assayed in the presence of 0.5 and 2 mM Nva or Val. Bacteria from 10 ml culture (OD_{600} = 0.2–0.6) were pelleted, resuspended in

0.5 ml buffer containing 4% SDS, 100 mM Tris–HCl (pH 8.0) and 10 mM EDTA and disrupted by sonication. The samples were heated 5 min at 95 °C and cleared by centrifugation. The proteins were precipitated using methanol/chloroform and resuspended in a denaturation buffer [6 M urea, 2 M thiourea and 10 mM Tris (pH 8.0)] as described [7].

Protein samples (10 µg of each) were digested in-solution [7]. Protein mixture was predigested with endoproteinase Lys-C (1:100 w/w) for 3 h, then diluted with 4 volumes of 20 mM ammonium bicarbonate (pH 8) and supplemented with trypsin (1:100 w/w) for overnight digestion at room-temperature.

LC–MS/MS measurement

Desalted and purified peptide samples (using C18 stage tips) [7] were separated by an EASY-nLC 1200 system (Thermo Scientific) coupled on-line to an Orbitrap Elite mass spectrometer (Thermo Scientific) through a nanoelectrospray ion source (Thermo Scientific). Chromatographic separation was performed on a 20-cm-long, 75-µm inner-diameter analytical column packed in-house with reversed-phase ReproSil-Pur C18-AQ 1.9-µm particles (Dr. Maisch GmbH). The column temperature was maintained at 40 °C using an integrated column oven. Peptides were loaded onto the column at a flow rate of 1 µl/min under maximum back-pressure of 850 bar. The peptides were eluted using 113-min linear gradient of 5%–33% solvent B at a constant flow rate of 200 nl/min. Peptides were ionized at 2.3 kV and the capillary temperature of 275 °C. The mass spectrometer was operated as previously described [7].

MS data processing and analysis

Acquired data (60 MS raw files) were processed using the MaxQuant software suite (version 1.5.2.8) [43]. Derived peak list was searched using Andromeda search engine integrated in MaxQuant [44] against a reference *E. coli* K12 proteome (taxonomy ID 83333) obtained from UniProt (4313 protein entries, released in October 2015) and a file containing 245 common laboratory contaminants implemented in MaxQuant. During the first search, peptide mass tolerance was set to 20 ppm and in the main search to 4.5 ppm. Ile substitution by Nva or Val was defined as variable modification with a loss of a CH_2 group (−14.0156500642 Da) at Ile position and named Ixx. Leu substitution by Nva or Val was searched alongside and was defined as variable modification with a loss of a CH_2 group (−14.0156500642 Da) at Leu position (Lxx). This was done as a control for the assignment of mistranslation because Ile and Leu are isobaric. Peptide, protein and modification site identifications were filtered using a target-decoy approach at FDR set to 0.01 [45]. We also used an unbiased protein modification search algorithm to verify that Nva and Val misincorporated with high localization accuracy at Ile positions (Supplementary Fig. S4) [7].

Frequencies of Val and Nva misincorporations were determined by spectral counting approach [7]. All contaminants and reverse hits were removed during data analysis. MS/MS spectra in msms.txt file were filtered for PEP scores of ≤ 0.01 and Andromeda score of ≥ 40. Only Nva/Val substitution events with a localization probability of ≥ 0.9 were considered as localized at Ile or Leu positions. The number of occurrences of Ixx substitutions were counted in Ixx-containing MS/MS spectra and divided by the number of theoretical isoleucine positions extracted from the unmodified version of peptide sequence of all MS/MS spectra. The same approach was used to determine mistranslation at Leu positions.

Bioinformatic analysis of shotgun proteomics data

Unique Ile positions were determined by assigning each measured peptide of the IleRS ED^- strain from the shotgun proteomics assay to Uniprot identifiers, and by identifying the location of the Ile residues in the primary sequence. This way, Ixx positions from the MS spectra were assigned to unique Ile positions in proteins. When comparing Val and Nva misincorporation positions, we restricted the dataset to peptides that were measured under all analyzed experimental conditions to avoid sampling bias of Ile positions. The probability to observe at least one misincorporation event at a given position is higher the more times the position was sampled (i.e., the frequency of its sampling in MS spectra). Therefore, we further limited the data set to peptides that were measured at least 4 times under all analyzed conditions (Supplementary Fig. S2). Three biological replicates of conditions F–G (Fig. 4) were merged. This resulted in data set of 827 unique peptides (having unique primary sequences) and corresponding to 1178 unique Ile positions (Supplementary Table S5). We tested the effect of different thresholds and the results did not change qualitatively; however, the more times an Ile position was sampled, the more Ile positions were identified as mistranslated and more overlap between Val and Nva mistranslation was found (Supplementary Fig. S3). Using four observations as a threshold, the number of measured peptides ranges from 5000 to 8000 for the different conditions (Supplementary Table S5). All analysis was performed using custom Python scripts.

Accession numbers

The MS proteomics data have been deposited to the ProteomeXchange Consortium (http://proteomecentral.proteomexchange.org/) *via* the PRIDE partner repository with the dataset identifier PXD011051 [46].

Acknowledgement

We thank Silke Wahl for her help in MS/MS sample preparation and Morana Dulic for participation in preliminary MS/MS analyses. D.S.T. is the Nella and Leon Benoziyo Professor of Biochemistry. This work was supported by the Croatian Science Foundation (Grant IP-2016-06-6272; to I.G.-S.). D.S.T. is funded by the Israel Science Foundation (Grant 980/14).

Author Contributions: M.B. performed some of *in vitro* analyses of IleRS and ValRS (Tables 1–3, Supplementary Tables S2 and S3); M.S. performed MS/MS analyses and MS/MS data interpretation under the guidance of B.M.; M.M. designed, measured and analyzed Nva and Val toxicity and prepared proteome samples for MS/MS analysis; I.Z. analyzed aminoacyl transfer by editing-deficient IleRS (Fig. 2) and performed some kinetic analyses (Tables 1 and 3); N.C. contributed to the design of *in vitro* experiments; D.S.T. contributed to developing evolutionary hypotheses and to writing of the manuscript; A.T.-P. performed computational analysis of MS/MS data; I.G.-S. designed the study, analyzed data and wrote the manuscript.

Appendix A. Supplementary data

Supplementary data to this article can be found online at https://doi.org/10.1016/j.jmb.2019.01.029.

Received 16 December 2018;
Received in revised form 20 January 2019;
Accepted 22 January 2019
Available online 31 January 2019

Keywords:
aminoacyl-tRNA synthetase;
mistranslation;
proofreading;
non-proteinogenic amino acids;
primordial translation

Present address: M. Bilus, Shire, Vienna 1220, Austria.

†The first three authors should be regarded as joint first authors.

Abbreviations used:
aa-AMP, aminoacyl-adenylate; aaRS, aminoacyl-tRNA synthetase; aa-tRNA, aminoacylated tRNA; CFU, colony-forming units; I/L/VRS, isoleucyl, leucyl, valyl-tRNA synthtetase; IleRS, isoleucyl-tRNA synthetase; LC–MS/MS, liquid chromatography–tandem mass spectrometry; LeuRS, leucyl-tRNA synthetase; MS, mass spectrometry; MS/MS, tandem mass spectrometry; Nva, norvaline; ValRS, valyl-tRNA synthetase; WT, wild-type.

References

[1] R.B. Loftfield, D. Vanderjagt, The frequency of errors in protein biosynthesis, Biochem. J. 128 (1972) 1353–1356, https://doi.org/10.1042/BJ1281353.
[2] E.B. Kramer, P.J. Farabaugh, The frequency of translational misreading errors in *E. coli* is largely determined by tRNA competition, RNA 13 (2007) 87–96, https://doi.org/10.1261/rna.294907.
[3] H. Jakubowski, Quality control in tRNA charging—editing of homocysteine, Acta Biochim. Pol. 58 (2011) 149–163, https://doi.org/10.1002/wrna.122.
[4] C.L. Linster, E. Van Schaftingen, A.D. Hanson, Metabolite damage and its repair or pre-emption, Nat. Chem. Biol. 9 (2013) 72–80, https://doi.org/10.1038/nchembio.1141.
[5] J. Soini, C. Falschlehner, C. Liedert, J. Bernhardt, J. Vuoristo, P. Neubauer, Norvaline is accumulated after a down-shift of oxygen in *Escherichia coli* W3110, Microb. Cell Factories 7 (2008) 30, https://doi.org/10.1186/1475-2859-7-30.
[6] E.R. Stadtman, R.L. Levine, Free radical-mediated oxidation of free amino acids and amino acid residues in proteins, Amino Acids 25 (2003) 207–218, https://doi.org/10.1007/s00726-003-0011-2.
[7] N. Cvetesic, M. Semanjski, B. Soufi, K. Krug, I. Gruic-Sovulj, B. Macek, Proteome-wide measurement of non-canonical bacterial mistranslation by quantitative mass spectrometry of protein modifications, Sci. Rep. 6 (2016), 28631. https://doi.org/10.1038/srep28631.
[8] T.J. Bullwinkle, N.M. Reynolds, M. Raina, A. Moghal, E. Matsa, A. Rajkovic, H. Kayadibi, F. Fazlollahi, C. Ryan, N. Howitz, K.F. Faull, B.A. Lazazzera, M. Ibba, Oxidation of cellular amino acid pools leads to cytotoxic mistranslation of the genetic code, elife 3 (2014), e02051. https://doi.org/10.7554/eLife.02501.001.
[9] J.J. Perona, I. Gruic-Sovulj, Synthetic and editing mechanisms of aminoacyl-tRNA synthetases, Top. Curr. Chem. 344 (2014) 1–41, https://doi.org/10.1007/128_2013_456.
[10] P. O'Donoghue, Z. Luthey-Schulten, On the evolution of structure in aminoacyl-tRNA synthetases, Microbiol. Mol. Biol. Rev. 67 (2003) 550–573, https://doi.org/10.1128/MMBR.67.4.550-573.2003.
[11] A.R. Fersht, Editing mechanisms in protein synthesis. Rejection of valine by the isoleucyl-tRNA synthetase, Biochemistry 16 (1977) 1025–1030, https://doi.org/10.1021/bi00624a034.
[12] M. Dulic, J.J. Perona, I. Gruic-Sovulj, Determinants for tRNA-dependent pretransfer editing in the synthetic site of isoleucyl-tRNA synthetase, Biochemistry 53 (2014) 6189–6198, https://doi.org/10.1021/bi5007699.
[13] L. Lin, S.P. Hale, P. Schimmel, Aminoacylation error correction, Nature 384 (1996) 33–34, https://doi.org/10.1038/384033b0.
[14] N. Cvetesic, M. Bilus, I. Gruic-Sovulj, The tRNA A76 hydroxyl groups control partitioning of the tRNA-dependent pre- and post-transfer editing pathways in class I tRNA synthetase, J. Biol. Chem. 290 (2015) 13981–13991, https://doi.org/10.1074/jbc.M115.648568.
[15] H.E. Umbarger, Amino acid biosynthesis and its regulation, Annu. Rev. Biochem. 47 (1978) 533–606, https://doi.org/10.1146/annurev.bi.47.070178.002533.
[16] V. Pezo, D. Metzgar, T.L. Hendrickson, W.F. Waas, S. Hazebrouck, V. Doring, P. Marliere, P. Schimmel, V. de Crecy-Lagard, Artificially ambiguous genetic code confers growth yield advantage, Proc. Natl. Acad. Sci. U. S. A. 101 (2004) 8593–8597, https://doi.org/10.1073/pnas.0402893101.

[17] J.O. Park, S.A. Rubin, Y.F. Xu, D. Amador-Noguez, J. Fan, T. Shlomi, J.D. Rabinowitz, Metabolite concentrations, fluxes and free energies imply efficient enzyme usage, Nat. Chem. Biol. 12 (2016) 482–489, https://doi.org/10.1038/nchembio.2077.
[18] K. Fujiwara, H. Toda, M. Ikeguchi, Dependence of α-helical and β-sheet amino acid propensities on the overall protein fold type, BMC Struct. Biol. 12 (2012) 18, https://doi.org/10.1186/1472-6807-12-18.
[19] P.C. Lyu, J.C. Sherman, A. Chen, N.R. Kallenbach, Alpha-helix stabilization by natural and unnatural amino acids with alkyl side chains, Proc. Natl. Acad. Sci. U. S. A. 88 (1991) 5317–5320, https://doi.org/10.1073/pnas.88.12.5317.
[20] N. Cvetesic, A. Palencia, I. Halasz, S. Cusack, I. Gruic-Sovulj, The physiological target for LeuRS translational quality control is norvaline, EMBO J. 33 (2014) 1639–1653, https://doi.org/10.15252/embj.201488199.
[21] I. Gruic-Sovulj, N. Uter, T. Bullock, J.J. Perona, tRNA-dependent aminoacyl-adenylate hydrolysis by a nonediting class I aminoacyl-tRNA synthetase, J. Biol. Chem. 280 (2005) 23978–23986, https://doi.org/10.1074/jbc.M414260200.
[22] N. Cvetesic, J.J. Perona, I. Gruic-Sovulj, Kinetic partitioning between synthetic and editing pathways in class I aminoacyl-tRNA synthetases occurs at both pre-transfer and post-transfer hydrolytic steps, J. Biol. Chem. 287 (2012) 25381–25394, https://doi.org/10.1074/jbc.M112.372151.
[23] M. Dulic, N. Cvetesic, J.J. Perona, I. Gruic-Sovulj, Partitioning of tRNA-dependent editing between pre- and post-transfer pathways in class I aminoacyl-tRNA synthetases, J. Biol. Chem. 285 (2010) 23799–23809, https://doi.org/10.1074/jbc.M110.133553.
[24] M. Yarus, P. Berg, Recognition of tRNA by isoleucyl-tRNA synthetase. Effect of substrates on the dynamics of tRNA-enzyme interaction, J. Mol. Biol. 42 (1969) 171–189, https://doi.org/10.1016/0022-2836(69)90037-0.
[25] A.C. Bishop, T.K. Nomanbhoy, P. Schimmel, Blocking site-to-site translocation of a misactivated amino acid by mutation of a class I tRNA synthetase, Proc. Natl. Acad. Sci. U. S. A. 99 (2002) 585–590, https://doi.org/10.1073/pnas.012611299.
[26] R. Fukunaga, S. Yokoyama, Structural basis for substrate recognition by the editing domain of isoleucyl-tRNA synthetase, J. Mol. Biol. 359 (2006) 901–912, https://doi.org/10.1016/j.jmb.2006.04.025.
[27] O. Khersonsky, D.S. Tawfik, Enzyme promiscuity: a mechanistic and evolutionary perspective, Annu. Rev. Biochem. 79 (2010) 471–505, https://doi.org/10.1146/annurev-biochem-030409-143718.
[28] A.L. Weber, S.L. Miller, Reasons for the occurrence of the twenty coded protein amino acids, J. Mol. Evol. 17 (1981) 273–284, https://doi.org/10.1007/BF01795749.
[29] C. Alvarez-Carreño, A. Becerra, A. Lazcano, Norvaline and norleucine may have been more abundant protein components during early stages of cell evolution, Orig. Life Evol. Biosph. 43 (2013) 363–375, https://doi.org/10.1007/s11084-013-9344-3.
[30] P. Schimmel, B. Henderson, Possible role of aminoacyl-RNA complexes in noncoded peptide synthesis and origin of coded synthesis, Proc. Natl. Acad. Sci. U. S. A. 91 (1994) 11283–11286, https://doi.org/10.1073/pnas.91.24.11283.
[31] Y. Pham, B. Kuhlman, G.L. Butterfoss, H. Hu, V. Weinreb, C.W. Carter, Tryptophanyl-tRNA synthetase urzyme: a model to recapitulate molecular evolution and investigate intramolecular complementation, J. Biol. Chem. 285 (2010) 38590–38601, https://doi.org/10.1074/jbc.M110.136911.
[32] L. Li, C. Francklyn, C.W. Carter, Aminoacylating urzymes challenge the RNA world hypothesis, J. Biol. Chem. 288 (2013) 26856–26863, https://doi.org/10.1074/jbc.M113.496125.
[33] L. Noda-Garcia, W. Liebermeister, D.S. Tawfik, Metabolite–enzyme coevolution: from single enzymes to metabolic pathways and networks, Annu. Rev. Biochem. 87 (2018) 187–216, https://doi.org/10.1146/annurev-biochem-062917-012023.
[34] N. Cvetešić, I. Akmačić, I. Gruić-Sovulj, Lack of discrimination against non-proteinogenic amino acid norvaline by elongation factor Tu from *Escherichia coli*, Croat. Chem. Acta 86 (2013) 73–82, https://doi.org/10.5562/cca2173.
[35] B. Zhu, P. Yao, M. Tan, G. Eriani, E.D. Wang, tRNA-independent pretransfer editing by class I leucyl-tRNA synthetase, J. Biol. Chem. 284 (2009) 3418–3424, https://doi.org/10.1074/jbc.M806717200.
[36] I. Gruic-Sovulj, J. Rokov-Plavec, I. Weygand-Durasevic, Hydrolysis of non-cognate aminoacyl-adenylates by a class II aminoacyl-tRNA synthetase lacking an editing domain, FEBS Lett. 581 (2007) 5110–5114, https://doi.org/10.1016/j.febslet.2007.09.058.
[37] K.E. Splan, M.E. Ignatov, K. Musier-Forsyth, Transfer RNA modulates the editing mechanism used by class II prolyl-tRNA synthetase, J. Biol. Chem. 283 (2008) 7128–7134, https://doi.org/10.1074/jbc.M709902200.
[38] Y. Song, H. Zhou, M.N. Vo, Y. Shi, M.H. Nawaz, O. Vargas-Rodriguez, J.K. Diedrich, J.R. Yates, S. Kishi, K. Musier-Forsyth, P. Schimmel, Double mimicry evades tRNA synthetase editing by toxic vegetable-sourced non-proteinogenic amino acid, Nat. Commun. 8 (2017), 2281. https://doi.org/10.1038/s41467-017-02201-z.
[39] G.M. Nagel, R.F. Doolittle, Phylogenetic analysis of the aminoacyl-tRNA synthetases, J. Mol. Evol. 40 (1995) 487–498 http://www.ncbi.nlm.nih.gov/pubmed/7783224 (accessed September 6, 2018).
[40] N. Cvetesic, I. Gruic-Sovulj, Synthetic and editing reactions of aminoacyl-tRNA synthetases using cognate and non-cognate amino acid substrates, Methods 113 (2017) 13–26, https://doi.org/10.1016/j.ymeth.2016.09.015.
[41] A.D. Wolfson, O.C. Uhlenbeck, Modulation of tRNAAla identity by inorganic pyrophosphatase, Proc. Natl. Acad. Sci. U. S. A. 99 (2002) 5965–5970, https://doi.org/10.1073/pnas.092152799.
[42] Q. Geissmann, OpenCFU, a new free and open-source software to count cell colonies and other circular objects, PLoS One 8 (2013), e54072. https://doi.org/10.1371/journal.pone.0054072.
[43] J. Cox, M. Mann, MaxQuant enables high peptide identification rates, individualized p.p.b.-range mass accuracies and proteome-wide protein quantification, Nat. Biotechnol. 26 (2008) 1367–1372, https://doi.org/10.1038/nbt.1511.
[44] J. Cox, N. Neuhauser, A. Michalski, R.A. Scheltema, J.V. Olsen, M. Mann, Andromeda: a peptide search engine integrated into the MaxQuant environment, J. Proteome Res. 10 (2011) 1794–1805, https://doi.org/10.1021/pr101065j.
[45] J.E. Elias, S.P. Gygi, Target-decoy search strategy for increased confidence in large-scale protein identifications by mass spectrometry, Nat. Methods 4 (2007) 207–214, https://doi.org/10.1038/nmeth1019.
[46] J.A. Vizcaíno, A. Csordas, N. Del-Toro, J.A. Dianes, J. Griss, I. Lavidas, G. Mayer, Y. Perez-Riverol, F. Reisinger, T. Ternent, Q.W. Xu, R. Wang, H. Hermjakob, 2016 update of the PRIDE database and its related tools, Nucleic Acids Res. 44 (2016) D447–D456, https://doi.org/10.1093/nar/gkv1145.